Abstract # 4788

Cross-validation between anti-CD3/CD8/FOXP3/pan-Cytokeratin fluorescent multiplex IHC and chromogenic single IHC by digital image analysis for quantifying tumor-infiltrating lymphocytes in colorectal cancer patient samples

Daniel Biljes*[1], Philipp Layer*[1], Nickels Winkler[1], Nadine Fändrich-Dursun[1], Cora Lohse[1], Hartmut Juhl[1], Kerstin David[1], Bernd Gromoll[1], Malik Khenkhar[1], Philipp C. Uhlig[1]
*contributed equally; [1]Indivumed GmbH, Hamburg, Germany

Background

A rising need for the overall goal to decipher cancer development and progression is a better understanding of the dynamics of the tumor microenvironment (TME), which are grounded in the interactions and reciprocal manipulation of cancer, stromal, and immune cells (Balkwill *et al.*, 2012). Tumor-infiltrating immune cells influence the TME, and analyses of immune cell types, densities and locations within the TME appears promising for establishing prognostic indicators and might help to identify more personalized anti-cancer therapies (Hanahan and Coussens, 2012). A new approach of analyzing the TME is the application of fluorescent multiplex immunohistochemistry (mIHC) and digital image analysis, but in order to be applied in the clinical setting the relevant assays require a precise validation.

Methods

Multiplex IHC: Tyramide signal amplification (TSA) based sequential fluorescent 5-color mIHC (CD8/ FOXP3/ CD3/ pCK + DAPI) of formalin-fixed paraffin-embedded (FFPE) colorectal cancer (CRC) tissue was implemented by Indivumed on the Leica BOND RX staining platform using the following antibody-fluorophore combinations: Anti-CD8 clone SP16 (DCS) and Opal 520 (PerkinElmer) (position 1), Anti-FOXP3 clone SP97 (ThermoFisher) and AF750 (ThermoFisher) (position 2), anti-CD3 clone 2GV6 (Roche) and Opal 690 (PerkinElmer) (position 3), as well as polyclonal anti-pan-Cytokeratin (pCK) (Dako, Z0622) and Opal 570 (PerkinElmer) (position 4). To determine staining conditions that ensure linearity, high sensitivity and low background a titration series of the primary antibodies was performed. The precision of multiplex-staining was analyzed by determining the within-run and between-run precision. To evaluate the within-run precision five serial sections of two CRC samples (A102-Tc12 and QG650-ET11) were immunohistochemically stained in one run (**Figure 4**). Furthermore, five serial sections of both validation controls were stained in five different runs to evaluate the between-run precision (**Figure 5**). Fifty human CRC samples (stage I: n = 13, stage II: n = 12, stage III: n = 12, stage IV: n = 13) were stained with the described mIHC panel and digital image analysis was performed (**Figure 7, Figure 8**).

Digital image analysis: Image analysis was performed with Visiopharm Oncotopix software. The optical analysis of chromogenic IHC by pathologist was used as a benchmark for digital image analysis. Tumor and stroma regions of interest (ROIs) were determined according to the pCK and DAPI signals (**Figure 6**). CD8, FOXP3 and CD3 single positive cells, as well as dual and triple positive cells, were then quantified in the tumor and stroma ROIs (**Figure 3**).

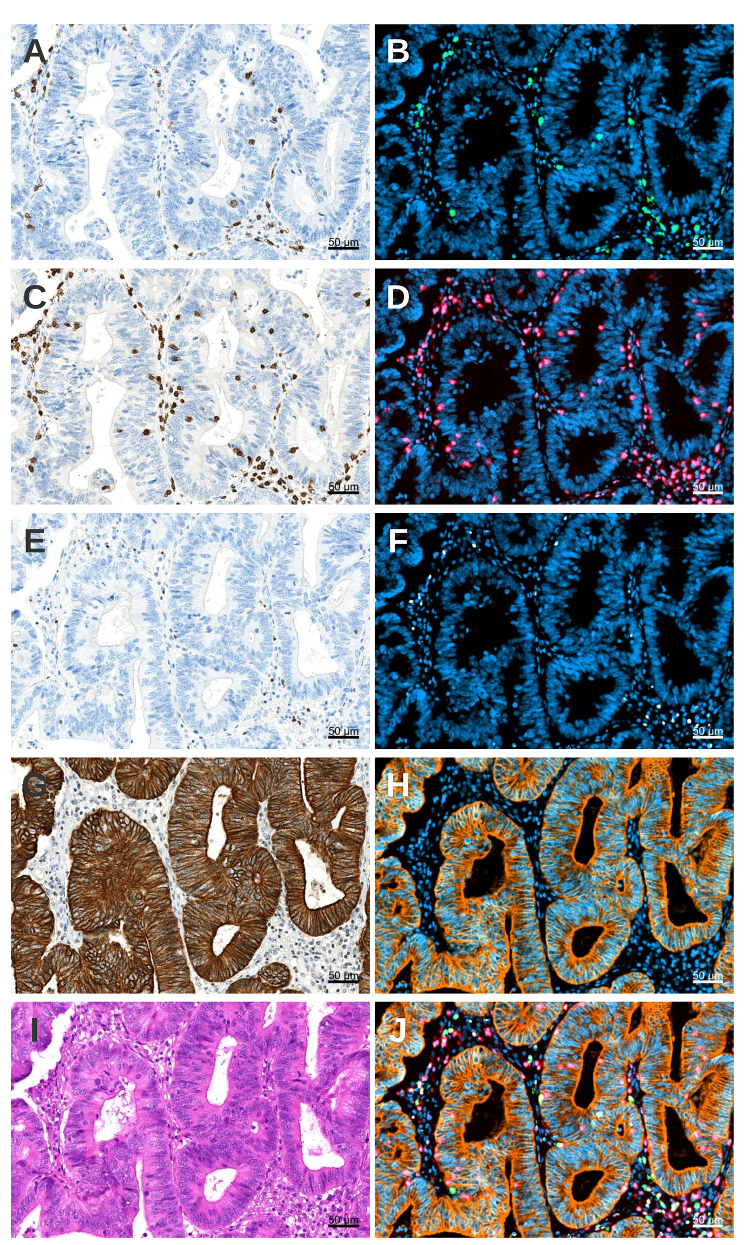

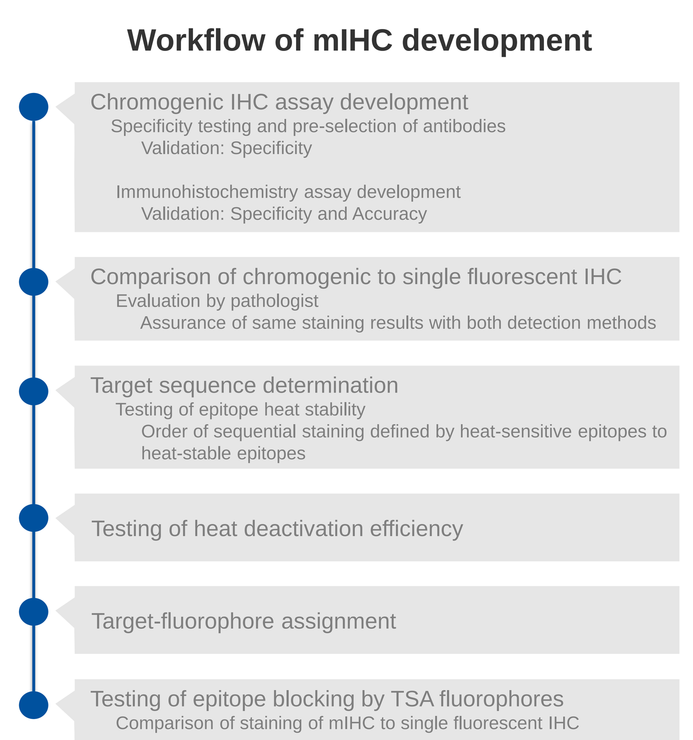

Figure 1: Comparison of chromogenic IHC and fluorescent mIHC of CRC tissue sample A102-Tc12. Four serial sections were stained by chromogenic single IHC for CD8, FOXP3, CD3 and pCK and one section was stained by mIHC with all antibodies. Anti-CD8 staining (**A**, brown; **B**, green). Anti-CD3 staining (**C**, brown; **D**, red). Anti-FOXP3 staining (**E**, brown; **F**, white). Anti-pCK staining (**G**, brown; **H**, orange). H&E staining (**I**). Anti-CD8/FOXP3/CD3/pCK mIHC staining (**J**, merge).

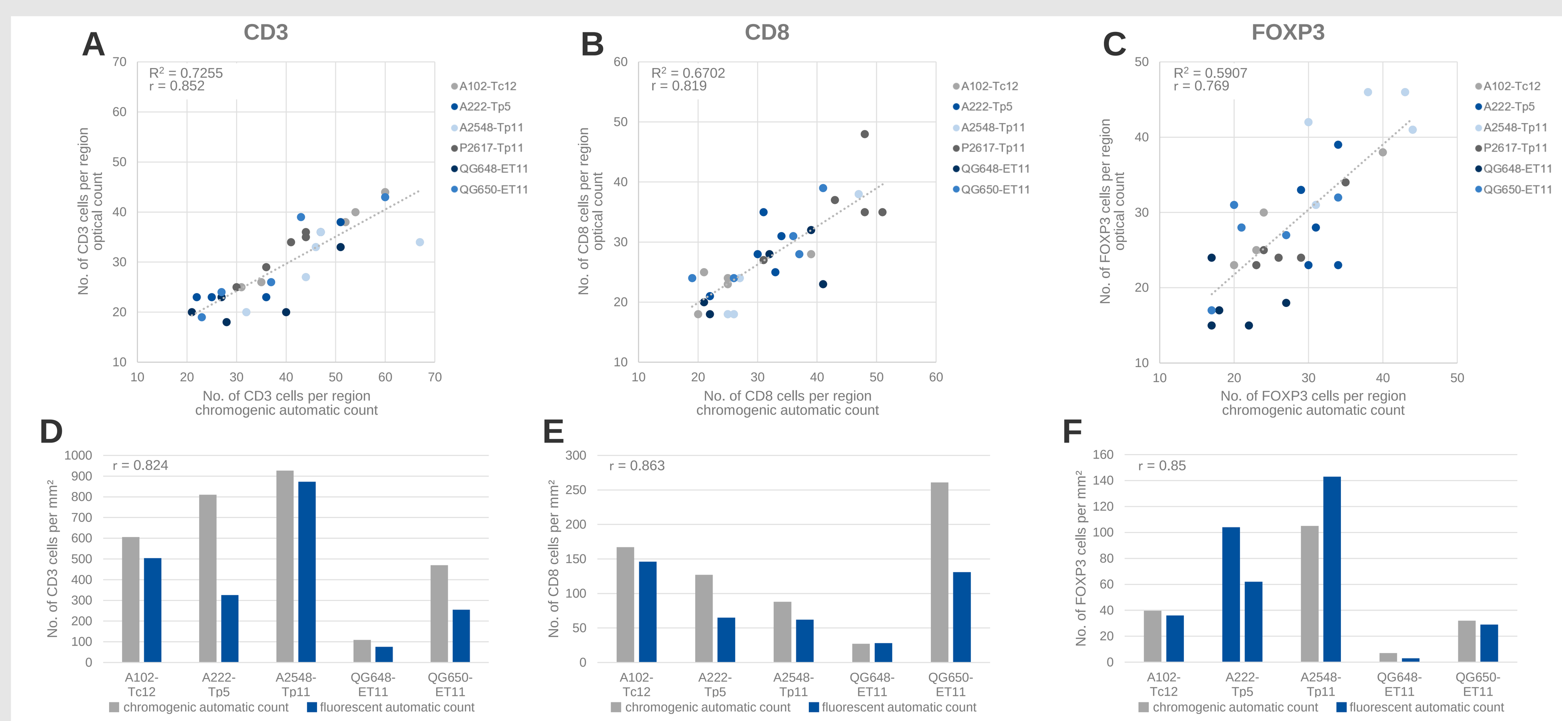

Figure 2: Comparison of optical analysis (Pathologist) to digital image analysis for chromogenic IHC (A-C) and of digital image analysis of chromogenic to fluorescent mIHC (D-F). A-C: The same five regions per sample were evaluated by pathologist (optical count) and by digital image analysis (automatic count) for CD3 (**A**), CD8 (**B**) and FOXP3 (**C**). **D-F:** Whole slide scans were analyzed by digital image analysis of chromogenic IHC or fluorescent mIHC of serial sections for CD3 (**D**), CD8 (**E**) and FOXP3 (**F**).

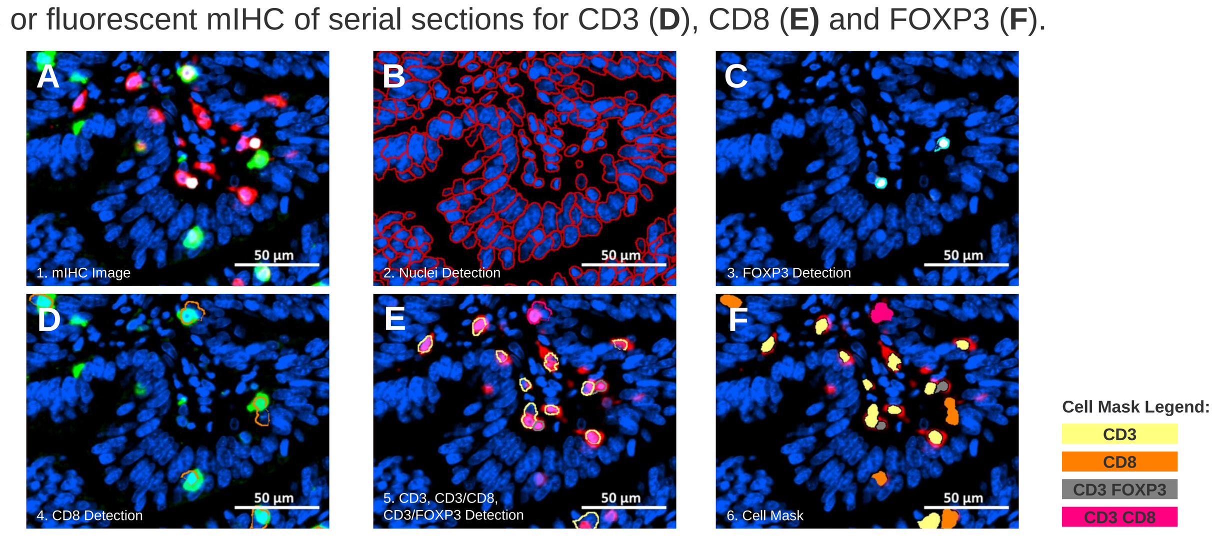

Figure 3: Digital image analysis algorithm. A: Original anti-CD3/CD8/FOXP3 staining (red/green/white). **B:** Nuclei detection (DAPI) and separation (red outlines). **C:** Detection of FOXP3 positive cells (white, cyan outlines). **D:** Detection of CD8 positive cells (green, orange outlines). **E:** Detection of CD3 positive (red, yellow outlines), CD3 CD8 dual positive (red, magenta outlines) and CD3 FOXP3 dual positive (red, gray outlines). **F:** Cellular image analysis overlay showing CD3 single (yellow overlay), CD8 single (orange overlay), CD3 CD8 dual (magenta overlay), and CD3 FOXP3 dual (gray overlay) positive cells.

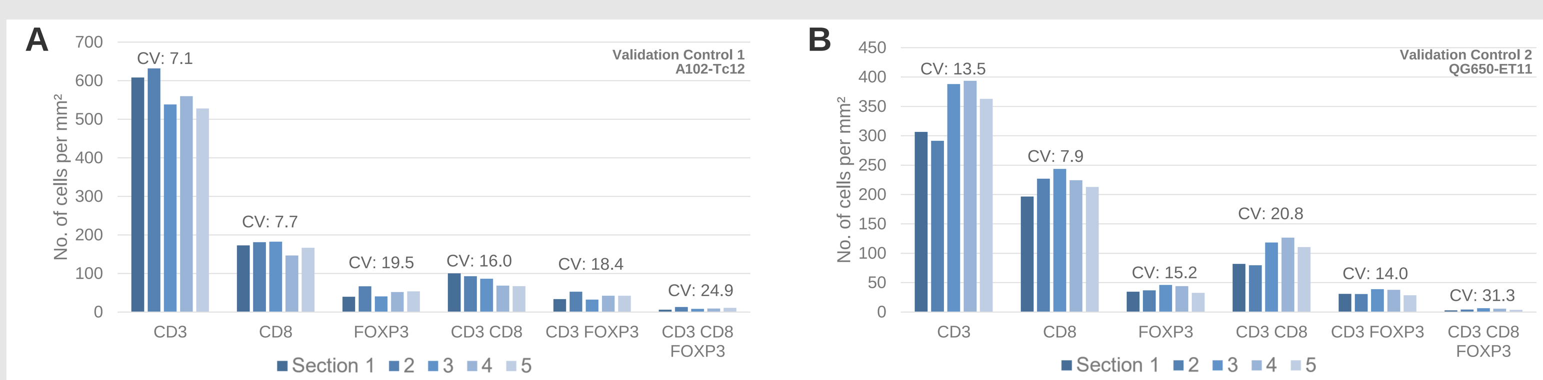

Figure 4: Within-run precision. Five serial sections of human FFPE CRC sample A102-Tc12 (**A**) and QG650-ET11 (**B**) were stained for CD8, FOXP3, CD3 and pCK in one staining run. Image analysis of whole slide scans was performed and numbers of counted immune cells were normalized to the analyzed areas. CV (%): Coefficients of variation in percent.

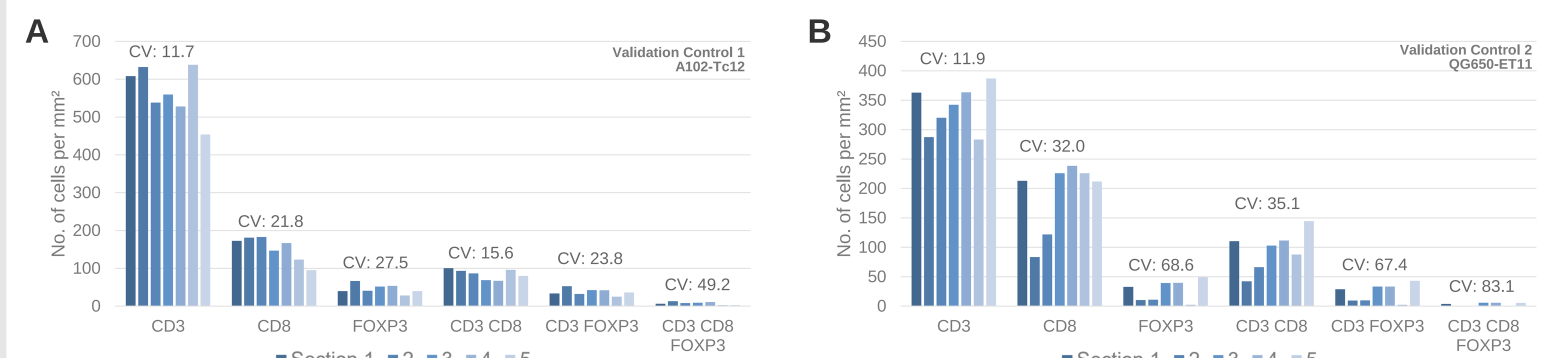

Figure 5: Between-run precision. Seven serial sections of human FFPE CRC sample A102-Tc12 (**A**) and QG650-ET11 (**B**) were stained for CD8, FOXP3, CD3 and pCK in seven different staining runs. Image analysis of whole slide scans was performed and the numbers of counted immune cells were normalized to the analyzed areas. CV (%): Coefficients of variation in percent.

Results

Good correlations were observed between optical analysis by pathologist and digital image analysis of chromogenic IHC, as well as between digital image analysis of chromogenic IHC or fluorescent mIHC ($r \geq 0.769$ Pearson correlation coefficient; **Figure 2**). A high within-run precision could be demonstrated for both validation control samples, with low cell densities being subject to higher variances (**Figure 4**). For the between-run precision, one validation control sample showed a comparably good repeatability, whereas the other sample showed a higher variance due to a weaker staining of two replicate slides. Furthermore, the distributions and ratios of the differently labeled tumor-infiltrating T cell populations in 50 CRC tissue samples as determined by fluorescent mIHC and digital image analysis (**Figure 3, Figure 6**) were in agreement with published literature (Pages *et al.*, 2005) and allowed for a classification of the samples regarding their infiltration by immune cells in the tumor or stroma ROI (**Figure 7, Figure 8**).

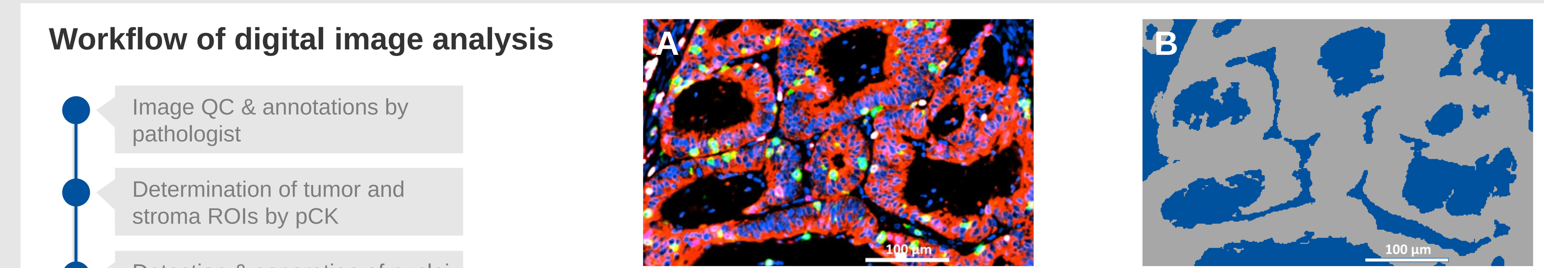

Figure 6: Determination of tumor and stroma ROIs by anti-pCK staining. A: Anti-CD8/FOXP3/CD3/pCK mIHC staining (CD8, green; FOXP3, white; CD3, red; pCK, orange). **B:** pCK mask overlay showing tumor (gray) and stroma (blue) ROIs.

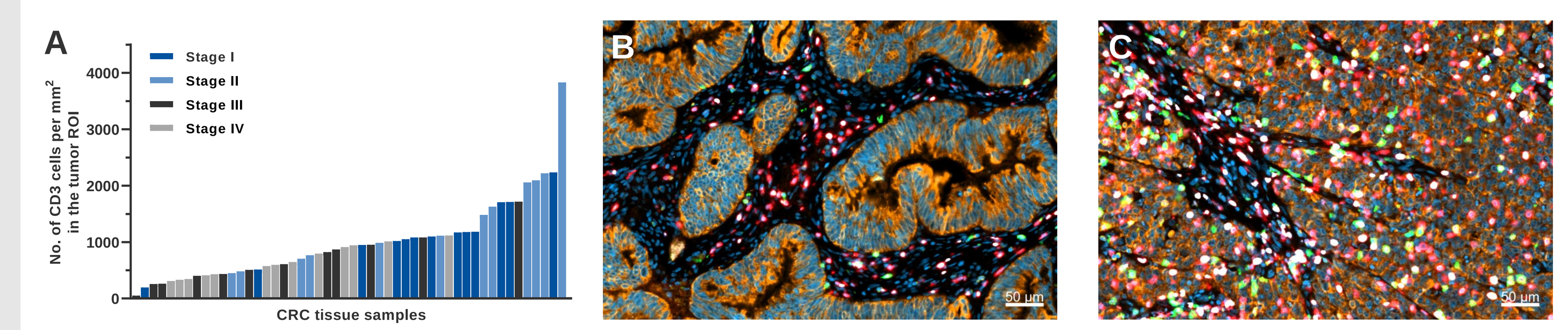

Figure 7: Anti-CD8/FOXP3/CD3/pCK mIHC of human FFPE CRC tissue samples. A: Measured densities of CD3 positive cells in the tumor ROI of all tested CRC samples sorted by density (stages are highlighted). **B, C:** Anti-CD8/FOXP3/CD3/pCK mIHC staining (CD8, green; FOXP3, white; CD3, red; pCK, orange) of a weakly infiltrated stage 4 CRC sample B1983-Tp14 (**B**) and strongly infiltrated, stage 2 CRC sample A4071-Tc316 (**C**).

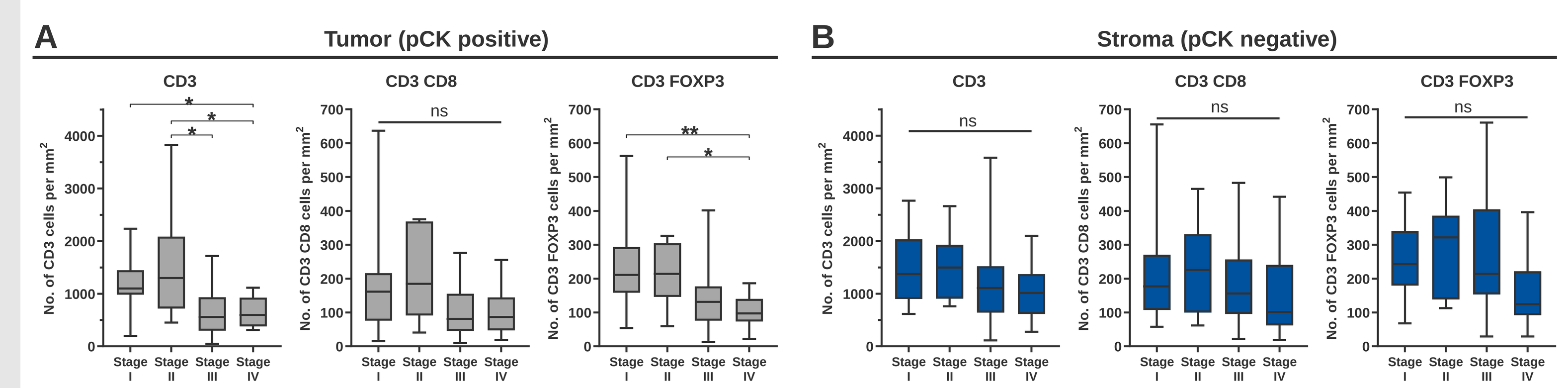

Figure 8: Proportions of CD3, CD3 CD8 and CD3 FOXP3 dual positive cell subsets in the tumor and stroma ROIs of 50 CRC tissue samples. A: In stage I or II tumors a significantly higher proportion of CD3 positive cells was observed than in samples of stage III or IV. No significant difference was observed for CD3 CD8 dual positive cells between the stages. A significantly higher proportion of CD3 FOXP3 dual positive cells was observed in samples of stage I or II than in samples of stage IV. **B:** No significant difference was observed in the stroma of CRC samples for CD3, CD3 CD8 or CD3 FOXP3 dual positive cells for the stages. (Statistical analysis by Dunn´s multiple comparison test; ns: P > 0.05, *: P ≤ 0.05, **: P ≤ 0.01).

Conclusion

The reliable quantification of immune cell subsets in FFPE CRC tissue samples shown here provides an efficient way of analyzing the lymphocyte composition of the TME at a validation level that is comparable to chromogenic IHC and apparently suitable for an application in the clinical setting. The validated combination of mIHC and digital image analysis may therefore enable a classification of the immune status of CRC patient samples and could help to identify new targets for anti-cancer therapy.

References:

Balkwill, F.R., Capasso, M., and Hagemann, T. (2012). The tumor microenvironment at a glance. Journal of cell science 125, 5591-5596.
Hanahan, D., and Coussens, L.M. (2012). Accessories to the crime: functions of cells recruited to the tumor microenvironment. Cancer Cell 21, 309-322.
Pages, F., Berger, A., Camus, M., Sanchez-Cabo, F., Costes, A., Molidor, R., Mlecnik, B., Kirilovsky, A., Nilsson, M., Damotte, D., et al. (2005). Effector memory T cells, early metastasis, and survival in colorectal cancer. The New England journal of medicine 353, 2654-2666

Scan me for Poster Download